



# UNIVERSITÀ DI PARMA

## ARCHIVIO DELLA RICERCA

University of Parma Research Repository

Formation of the Huajiang Grand Canyon (southwestern China) driven by the evolution of a Late Pleistocene tiankeng

This is the peer reviewed version of the following article:

*Original*

Formation of the Huajiang Grand Canyon (southwestern China) driven by the evolution of a Late Pleistocene tiankeng / Fan, Yunlong; Columbu, Andrea; Xiong, Kangning; Luo, Guangjie; Li, Song; Wang &, Xuefeng; Wu, Yangyang. - In: ACTA GEOCHIMICA. - ISSN 2365-7499. - (2022).

*Availability:*

This version is available at: 11381/2914770 since: 2022-05-02T11:56:50Z

*Publisher:*

*Published*

DOI:

*Terms of use:*

Anyone can freely access the full text of works made available as "Open Access". Works made available

*Publisher copyright*

note finali coverpage

(Article begins on next page)

10 April 2024

# Metadata of the article that will be visualized in OnlineFirst

ArticleTitle	Formation of the Huajiang Grand Canyon (southwestern China) driven by the evolution of a Late Pleistocene tiankeng		
Article Sub-Title			
Article CopyRight	The Author(s), under exclusive licence to Science Press and Institute of Geochemistry, CAS and Springer-Verlag GmbH Germany, part of Springer Nature (This will be the copyright line in the final PDF)		
Journal Name	Acta Geochimica		
Corresponding Author	FamilyName	<b>Fan</b>	
	Particle		
	Given Name	<b>Yunlong</b>	
	Suffix		
	Division	Key Laboratory of Western China’s Environmental Systems (Ministry of Education), College of Earth and Environmental Sciences	
	Organization	Lanzhou University	
	Address	Lanzhou, 730000, Gansu, China	
	Division	Guizhou Provincial Key Laboratory of Geographic State Monitoring of Watershed, School of Geography and Resource Science	
	Organization	Guizhou Education University	
	Address	Guiyang, 550018, Guizhou, China	
	Phone		
	Fax		
	Email	fanyl14@lzu.edu.cn	
	URL		
ORCID	http://orcid.org/0000-0002-0671-7075		
Corresponding Author	FamilyName	<b>Xiong</b>	
	Particle		
	Given Name	<b>Kangning</b>	
	Suffix		
	Division	School of Karst Science	
	Organization	Guizhou Normal University	
	Address	Guiyang, 550001, Guizhou, China	
	Phone		
	Fax		
	Email	xiongkn@163.com	
	URL		
	ORCID		
	Author	FamilyName	<b>Columbu</b>
		Particle	
Given Name		<b>Andrea</b>	
Suffix			
Division		Department of Chemistry, Life Sciences and Environmental Sustainability	
Organization		University of Parma	
Address		43124, Parma, Italy	
Phone			
Fax			
Email			
URL			
ORCID			

Author	FamilyName	<b>Luo</b>
	Particle	
	Given Name	<b>Guangjie</b>
	Suffix	
	Division	Guizhou Provincial Key Laboratory of Geographic State Monitoring of Watershed, School of Geography and Resource Science
	Organization	Guizhou Education University
	Address	Guiyang, 550018, Guizhou, China
	Phone	
	Fax	
	Email	
	URL	
	ORCID	
Author	FamilyName	<b>Li</b>
	Particle	
	Given Name	<b>Song</b>
	Suffix	
	Division	Guizhou Provincial Key Laboratory of Geographic State Monitoring of Watershed, School of Geography and Resource Science
	Organization	Guizhou Education University
	Address	Guiyang, 550018, Guizhou, China
	Phone	
	Fax	
	Email	
	URL	
	ORCID	
Author	FamilyName	<b>Wang</b>
	Particle	
	Given Name	<b>Xuefeng</b>
	Suffix	
	Division	Key Laboratory of Cenozoic Geology and Environment, Institute of Geology and Geophysics
	Organization	Chinese Academy of Sciences
	Address	Beijing, 100029, China
	Phone	
	Fax	
	Email	
	URL	
	ORCID	
Author	FamilyName	<b>Wu</b>
	Particle	
	Given Name	<b>Yangyang</b>
	Suffix	
	Division	Guizhou Provincial Key Laboratory of Geographic State Monitoring of Watershed, School of Geography and Resource Science
	Organization	Guizhou Education University
	Address	Guiyang, 550018, Guizhou, China
	Phone	
	Fax	
	Email	
	URL	
	ORCID	
Schedule	Received	9 Sep 2021
	Revised	28 Oct 2021
	Accepted	31 Oct 2021
Abstract	<p>Collapse is a common geomorphic process in karst areas, especially on the Yunnan-Guizhou Plateau, which has a tectonic background of integral uplift. The frequent occurrence of collapse processes in karst underground caves and canyons indicates that collapses play an important role in the formation of canyons. Through an analysis of the morphology of a semicircular cliff in the Huajiang Grand Canyon and an investigation of sediments at the bottom of the cliff, a large-scale collapse event was found to have occurred. U-series dating of secondary calcium carbonate cement in the collapse breccias indicates that collapse processes occurred approximately 200 ka. According to the geomorphological evolution of the Huajiang Grand Canyon, the following geomorphic evolutionary process is proposed: underground river—cave hall—collapse of a tiankeng—tiankeng degradation—canyon formation. These findings also show that the dating of collapsed breccia cement can be effectively used to determine the development times of karst canyons and the formation ages of tiankengs.</p>	







# Formation of the Huajiang Grand Canyon (southwestern China) driven by the evolution of a Late Pleistocene tiankeng

Yunlong Fan<sup>1,2</sup> · Andrea Columbu<sup>3</sup> · Kangning Xiong<sup>4</sup> · Guangjie Luo<sup>2</sup> · Song Li<sup>2</sup> · Xuefeng Wang<sup>5</sup> · Yangyang Wu<sup>2</sup>

Received: 9 September 2021 / Revised: 28 October 2021 / Accepted: 31 October 2021

© The Author(s), under exclusive licence to Science Press and Institute of Geochemistry, CAS and Springer-Verlag GmbH Germany, part of Springer Nature 2021

**Abstract** Collapse is a common geomorphic process in karst areas, especially on the Yunnan-Guizhou Plateau, which has a tectonic background of integral uplift. The frequent occurrence of collapse processes in karst underground caves and canyons indicates that collapses play an important role in the formation of canyons. Through an analysis of the morphology of a semicircular cliff in the Huajiang Grand Canyon and an investigation of sediments at the bottom of the cliff, a large-scale collapse event was found to have occurred. U-series dating of secondary calcium carbonate cement in the collapse breccias indicates that collapse processes occurred approximately 200 ka. According to the geomorphological evolution of the Huajiang Grand Canyon, the following geomorphic

evolutionary process is proposed: underground river—cave hall—collapse of a tiankeng—tiankeng degradation—canyon formation. These findings also show that the dating of collapsed breccia cement can be effectively used to determine the development times of karst canyons and the formation ages of tiankengs.

AQ1

## 1 Introduction

Canyons are peculiar landscape morphologies produced by multiple processes (Hill et al. 2008; Karlstrom et al. 2014; Wang et al. 2014). Canyons form in different lithologies, but they are often found in karst terrains (Ford 1973; Abbott et al. 2015; Telbiszet al. 2019). Because karst allows underground drainage, river banks are not significantly eroded, and steep slopes are preserved. Therefore, deep canyons are a common and remarkable feature of karstic landscapes (Sweeting 1995). In uplifting areas, rivers progressively cut across landforms (Nicod 1997); thus, the development of deep canyons is controlled by the base level (Fabre and Nicod 1978). Another key factor in the development of canyons is gradually deepening from the lower to upper reaches of valleys, which is driven by the migration of the knickpoint (Germanoski and Ritter 1988; Hu et al. 2016). However, in karst terrains, cave collapse also plays a significant role (Nicod 1997).

The Yunnan-Guizhou Plateau (Southwest China) has been uplifted since the Cenozoic (Tapponnier 2001; Clark et al. 2006) due to the uplift of the Qinghai-Tibetan Plateau. The rapid uplift of this extensive Chinese karst region has favoured underground drainage and thus the formation of caves. The expansion of underground spaces (lateral and/or vertical expansion) eventually leads to the collapse

✉ Yunlong Fan  
fanyl14@lzu.edu.cn

✉ Kangning Xiong  
xiongkn@163.com

<sup>1</sup> Key Laboratory of Western China's Environmental Systems (Ministry of Education), College of Earth and Environmental Sciences, Lanzhou University, Lanzhou 730000, Gansu, China

<sup>2</sup> Guizhou Provincial Key Laboratory of Geographic State Monitoring of Watershed, School of Geography and Resource Science, Guizhou Education University, Guiyang 550018, Guizhou, China

<sup>3</sup> Department of Chemistry, Life Sciences and Environmental Sustainability, University of Parma, 43124 Parma, Italy

<sup>4</sup> School of Karst Science, Guizhou Normal University, Guiyang 550001, Guizhou, China

<sup>5</sup> Key Laboratory of Cenozoic Geology and Environment, Institute of Geology and Geophysics, Chinese Academy of Sciences, Beijing 100029, China

of caves. On the Guizhou Plateau, the collapse of underground river passages is very common (Zhang and Mo 1982; Sweeting 1995; Szczygiel et al. 2018), often causing the opening of the chamber roof to the ground surface. Several morphologies in this area (i.e., large depressions, canyons, valleys, cones, and tower karst) are attributed to cave collapse (Ambert and Nicod 1981; Alexander 2005), including tiankengs. The latter are giant collapse dolines with continuous precipitous walls (Alexander 2005; Zhu and Chen 2005; Waltham 2015; Michelena 2020). In most cases, the accumulation of colluvium can be observed at the bottom of tiankengs. According to the evolution of similar landforms, large underground rivers are prone to collapse, thus forming tiankengs. The Xingwen Tiankeng group in Sichuan (Waltham 2005), Wulong Tiankeng group in Chongqing (Alexander 2005; Szczygiel et al. 2018), and Leye Tiankeng group in Guangxi (Zhu and Waltham 2005) are other examples of tiankengs. Many tiankengs are also distributed on the tributaries of large rivers on the plateau. For example, the Dacaoou and Xiaocaoou Tiankengs on the Yijie River, which is a tributary of the Wujiang River, and the Jiudongtian Tiankeng on the Liuchong River in the upper reaches of the Wujiang River are narrow, long tiankengs formed by collapsed cave passages (An et al. 2019). These tiankengs represent the embryonic form in the evolution from tiankeng to canyon.

The shape of tiankengs evolves because of the lateral expansion of the walls and collapses. If these karst-related features endure through time, the original morphology is obliterated. Thus, understanding the evolution of a karst area where tiankengs have reached a mature stage might be difficult. As for all morphologies related to underground voids (Sasowsky 1998), determining the age of tiankengs is complicated (Shui et al. 2015). There have been several attempts to determine the chronological evolution of these landforms in China using different approaches. According to geological observations, Zhu and Chen (2005) speculated that most tiankengs in China formed since the Late Pleistocene, while Wei et al. (2019) inferred that Fengjie Tiankeng was formed in the late Middle Pleistocene. Meng et al. (2017) also determined that the exposure age of Dashiwei Tiankeng is at least 100–200 ka BP based on bedrock cosmogenic  $^{36}\text{Cl}$  exposure dating. Therefore, more exhaustive information about the age and evolution of these morphologies is needed.

Cave deposits can be dated to infer the ages of caves (Polyak et al. 2008; Granger and Fabel 2012; Anthony 2012; Columbu et al. 2021). Chemically precipitated carbonate (i.e., speleothems) is an ideal candidate because U-series dating of calcite is very efficient (Cheng et al. 2016). Importantly, speleothems are deposited after cave formation (Wang et al. 2004; Columbu et al. 2015) in either

subaerial or submerged conditions (De Waele et al. 2018). Speleothems found at the surface indicate that the original hosting cave has been disrupted (Columbu et al. 2017).

This paper investigates the evolution of the Huajiang Grand Canyon on the Guizhou Plateau in the middle reaches of the Beipan River. Geomorphological observations suggest the presence of a relict tiankeng, and secondary carbonate dating was applied to deposits previously formed in underground environments. Accordingly, this paper aims to reconstruct the genesis of the current canyon relative to the maturation of the relict tiankeng, placing this karst-related process into a congruent geochronological timeframe.

## 2 Area of study

The Beipan River originates from the eastern part of Yunnan Province and flows from northwest to southeast across the Yunnan–Guizhou Plateau (Fig. 1A–B). Reaching the slopes of Guangxi, this river is 449 km long with a drop of 1982 m, corresponding to an average drop of 4.42‰, and has a catchment area of 25,830 km<sup>2</sup> (Fan et al. 2018). Wide varieties of rocks are exposed in the basin, including a large number of soluble rocks, such as Devonian, Carboniferous, Permian, Triassic limestone, and dolomite, as well as nonsoluble rocks, such as siltstone and mudstone.

Under the influence of lateral extrusion from the southeastern Qinghai–Tibetan Plateau, the Yunnan–Guizhou Plateau has undergone differential uplift alongside the uplift of the Qinghai–Tibetan Plateau. Low-relief and high-elevation surfaces are broadly distributed, elevation decreases gradually from the northwest to the southeast, and western plateau surfaces with altitudes of 2100–2200 m and eastern plateau surfaces with altitudes of 1300–1400 m are relatively intact (Clark et al. 2006). The valleys of the Beipan River and its tributaries are deep, and the plateau is divided by numerous rivers. The surface has experienced extensive erosion, resulting in a shortage of widespread, continuous Quaternary sediments (Liu et al. 2013).

The Huajiang Canyon is located in the middle reaches of the Beipan River, 5 km upstream from Huajiang village (Fig. 1). Covering a total length of 30 km (Fig. 1C), the canyon coincides with the Zhenfeng Fault. On the western side of the fault, a well-preserved karst plateau surface is maintained, with an average elevation of 1300–1400 m (Fig. 1D). On the eastern side of the fault, the terrain is relatively low with no intact plateau surface, forming a hilly country with an elevation of 500–1000 m. With the fault as the boundary, the lower reaches of the river are open, and the river becomes sluggish, while the upper

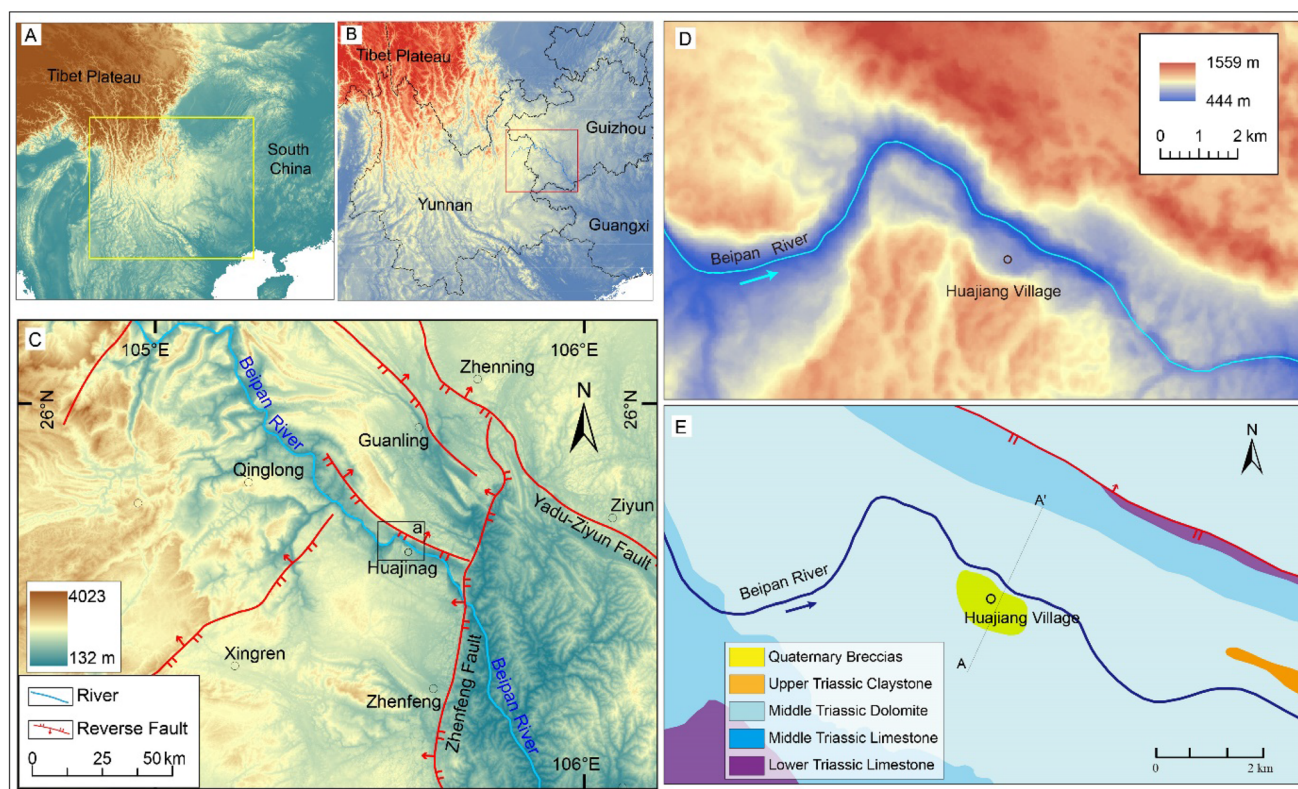


**Fig. 1** Study area. **A** Location of the Yunnan–Guizhou Plateau. **B** Location of the Beipan River. **C** Digital elevation model of Huajiang Canyon and surrounding areas, with the main fault system shown. **D** Digital elevation model of the Huajiang Canyon area. **E** Simplified geologic map of Huajiang Canyon (section A–A' is shown in Fig. 3a)

reaches exhibit deep canyons. In the section containing Huajiang village, the vertical drop of the canyon is very large, with a depth of approximately 800–1000 m. In this section, the river cuts deeply into the dolomite strata of the Triassic Yangliujing Formation. In the study area, the canyons consist of an ~ 3-km-wide outer canyon and an ~ 150-m-wide inner canyon with a depth of 200 m. The two sides of Huajiang Canyon are surrounded by plateau surfaces, with several 100–200 m-high fengcongs present (Fig. 1D).

Within Huajiang Canyon, a distinct platform is identified (25°41'52"N, 105°35'24"E). The elevation of this platform is higher than that of the modern river channel by approximately 200 m (Fig. 2A). The altitude of the platform is approximately 700 m, and the elevation of the bed of the Beipan River is 500 m. A semicircular vertical cliff is retained on the side of the canyon where the Huajiang platform is located. Furthermore, some residual peaks occur on the opposite bank of the canyon. A large amount of karst breccia has been deposited on the platform of Huajiang village, with a thickness of 5–10 m. The bedrock beneath the breccias is an ancient cave floor. In addition, many remains of ancient stalagmites were observed on the Huajiang platform (Fig. 3).

### 3 Materials

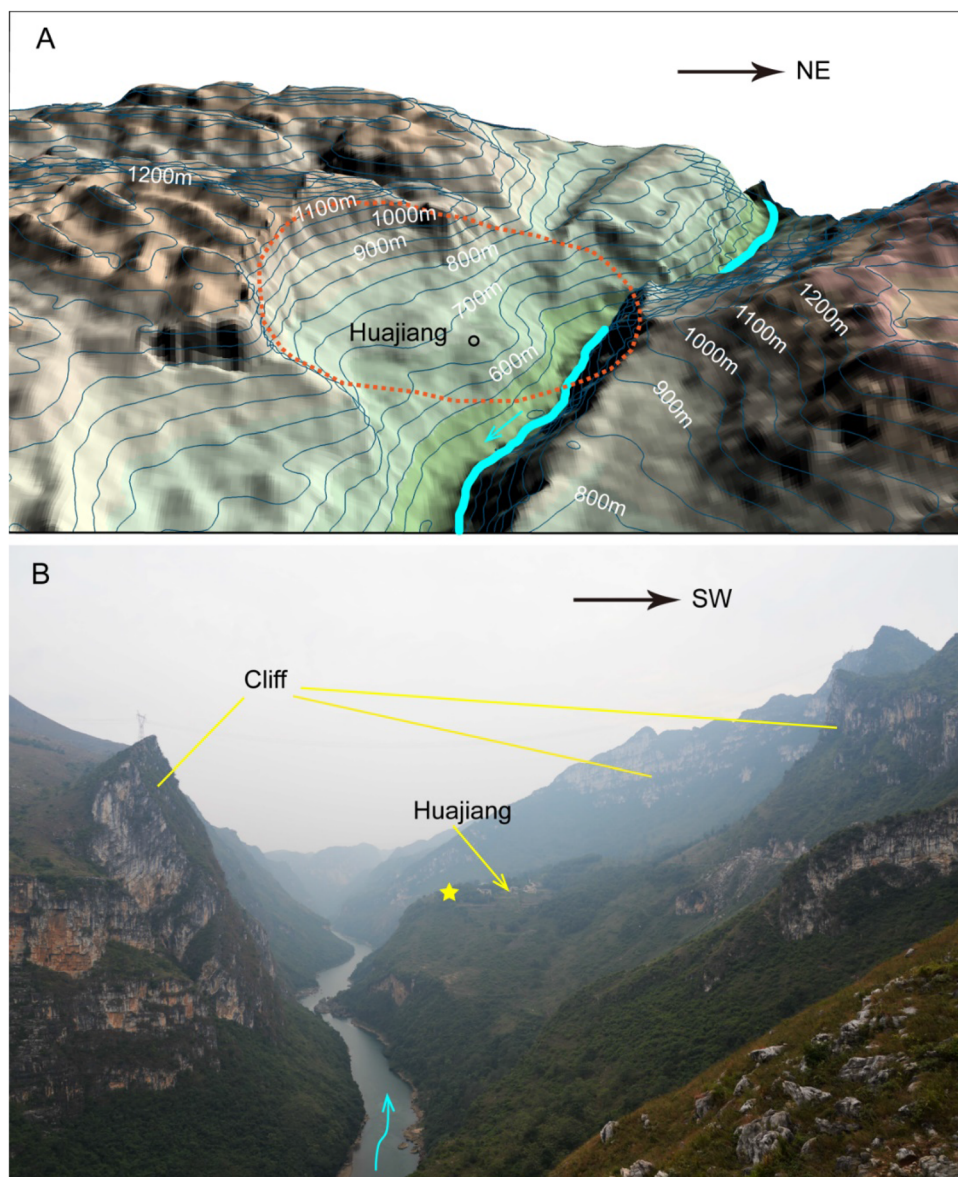
The breccias on the Huajiang platform are composed of dolomites, have a mixed structure with no obvious bedding, and are densely cemented by secondary calcium carbonate (Fig. 3c–j). According to their sedimentary characteristics, they can be identified as colluvial breccias with a thickness of 5–10 m. Many remains of ancient stalagmites were observed on the Huajiang platform. Some stalagmites remain upright, with dolomite bedrock at the bottom (Fig. 3l). Some of the damaged stalagmites are buried in the soil (Fig. 3k). Although all of the stalagmites were eroded and weathered under the soil in the later stage, laminae and morphological characteristics can be identified in the fracture section.

Four secondary calcium carbonate deposits on the Huajiang platform were investigated (Fig. 3), two of which were breccia samples (BHJT2 and BHJT4): BHJT2 located at the bottom of the tiankeng (695 m a.s.l.) and BHJT4 located on the slope at the edge of the tiankeng (780 m a.s.l.). The remaining samples (BHJT3BS and BHJT3CS) were two ancient stalagmites on the Huajiang platform. Samples for dating were obtained from the top and bottom of each stalagmite. Fortunately, freshly exposed breccias



**Fig. 2** **A** 3D topographic map of Huajiang Canyon. The orange dotted line indicates the shape of the original tiankeng.

**B** Photo of the degraded Huajiang Tiankeng, looking southeast. The yellow lines point to the remaining cliffs from the collapse



could be observed in a slope section excavated during the construction of a road leading to Huajiang village. The breccias were well cemented and compact. Sample BHJT2 was collected beside the road (695 m a.s.l.) from a location 1.8 m below the top surface of the breccias. Sample BHJT4 was collected beside the road (780 m a.s.l.) from a location 3 m below the top of the profile. Sampling targeted locations potentially repaired after post-depositional weathering. Samples were detached from the original surface using a hammer and chisel. Thin sections of all breccia samples were prepared for petrographic investigation (Fig. 3f, g–i, j).

## 4 Methods

Petrographic thin sections were investigated using a Leica DM4500P polarizing microscope. Subsamples weighing approximately 50–100 mg were collected for U–Th dating by drilling along the growth layers using a dental hand drill. Dating was performed to attempt to establish the ages of the stalagmites and colluvium cementation to constrain the time(s) of the collapse event(s). When the bottom or top of a stalagmite was considered unsuitable for dating due to obvious clastic material in the laminae, samples of the closest clean and unaltered calcite were collected.

The uranium-series dating method is an effective dating method for determining geological age based on the disequilibrium between radionuclide  $^{238}\text{U}$  and its decay daughters  $^{234}\text{U}$  and  $^{230}\text{Th}$  (Edwards et al. 1987). Using

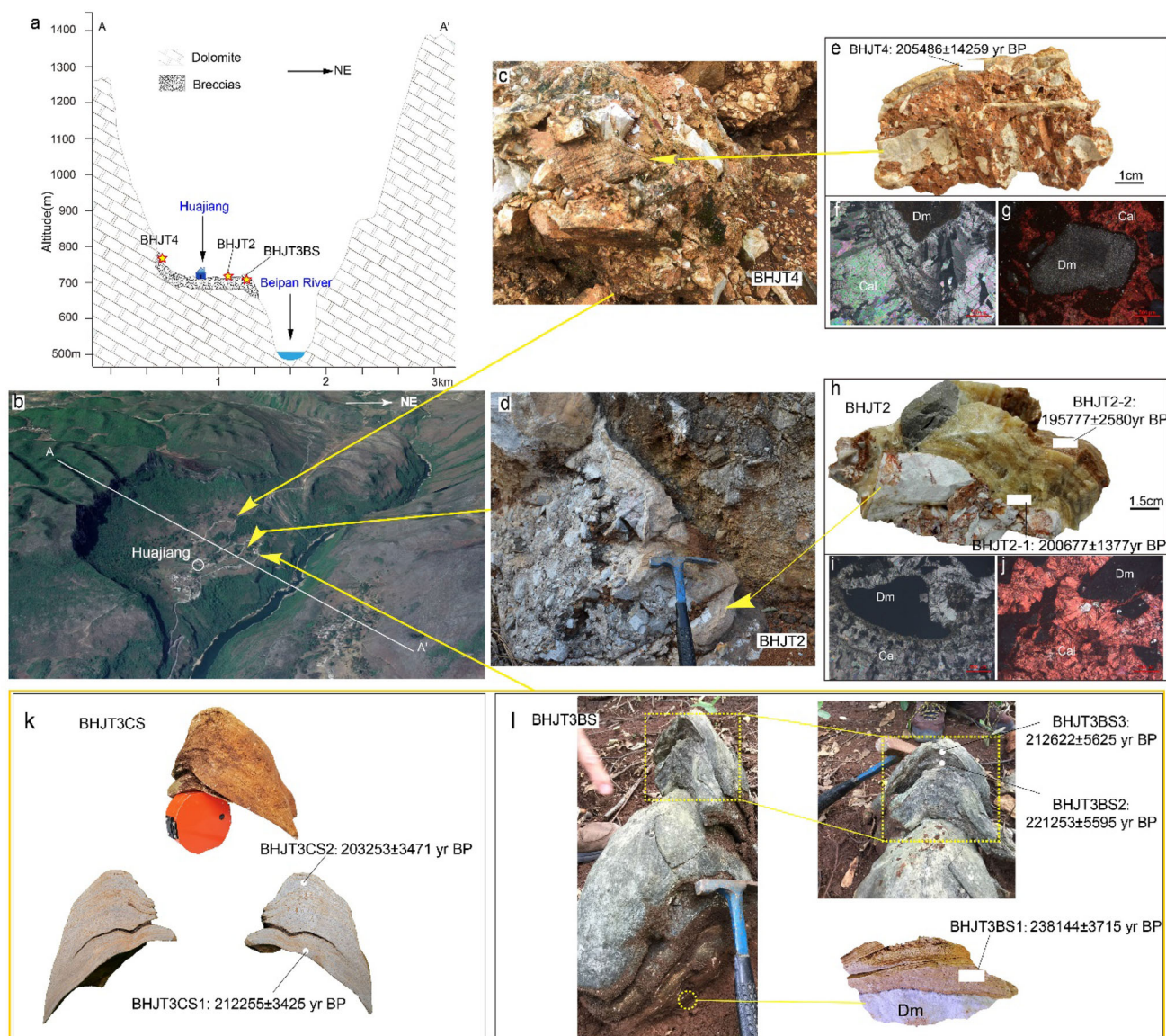


**Fig. 3** **a** Huajiang Tiankeng profile. Its position is coincident with the dashed line (A–A') in Fig. 1E. The yellow stars indicate sampling locations. **b** Satellite image (from Google Earth) showing the degraded Huajiang Tiankeng. The yellow arrows indicate the sampling locations. **c** Karst breccias (BHJT4) deposited in the slope area at the edge of the Huajiang Tiankeng. **d** Karst breccias (BHJT2), deposited at the bottom of the Huajiang Tiankeng. **e** Hand specimen, BHJT4. **f–g** Microphotographs of BHJT4. **h** Hand specimen, BHJT2. **i–j** Microphotographs of BHJT2. **k** Stalagmite buried under the soil and its longitudinal section. Crack formation due to dissolution under the soil is visible in the longitudinal section of the stalagmite. **l** Stalagmites exposed on the Earth's surface and their ages (the stalagmites are grown on the dolomite bedrock, and samples for dating were collected from the bottom of the stalagmites). The locations of these residual stalagmites **k–l** are shown by yellow stars in Fig. 2B (Dm represents dolomite, and Cal represents calcite)

multicollector–inductively coupled plasma–mass spectrometry (MC–ICP–MS), the U–Th dating method provides a dating range from decades to 640 ka (Cheng, 2013). U–Th dating was performed at the Uranium Series Chronology Laboratory of the Institute of Geology and Geophysics at the Chinese Academy of Sciences in Beijing. Chemical treatment was performed following the Edwards method (Edwards et al. 1987; Wang et al. 2017). The subsamples were first dissolved in  $\text{HNO}_3$ , followed by the addition of a

few drops of  $\text{HClO}_4$ . All samples were spiked with a  $^{229}\text{Th}$ – $^{233}\text{U}$ – $^{236}\text{U}$  tracer (Chen et al. 1986; Shen et al. 2002; Cheng et al. 2013). The mixed solutions were placed on a 150 °C hot plate for 5–10 h and evaporated to dryness. Then, the samples were dissolved in 2 M HCl and transferred to clean centrifuge tubes. Approximately 10 mg of  $\text{FeCl}_3$  was added and mixed, followed by a few drops of  $\text{NH}_3\cdot\text{H}_2\text{O}$  to adjust the pH to 7–8. In this step, a slightly reddish-brown  $\text{Fe}(\text{OH})_3$  precipitate was formed, with



simultaneous coprecipitation of U and Th from the mixed liquids. The precipitates were washed twice with ultrapure water, dissolved in 0.5 mL 7 M HNO<sub>3</sub>, and dried again at 150 °C. Then, the samples were dissolved in 7 M HNO<sub>3</sub> and loaded onto 7 M HNO<sub>3</sub>-conditioned anion-exchange columns. Trace metal elements were eluted with 7 M HNO<sub>3</sub>, Th was eluted with 8 M HCl, and U was eluted with 0.1% HNO<sub>3</sub>. The U and Th fractions were dried at 150 °C and dissolved in 2% HNO<sub>3</sub> + 0.1% HF. The U and Th recovery in this procedure was higher than 90%. The half-lives of <sup>234</sup>U and <sup>230</sup>Th were determined based on data proposed by Cheng et al. (2013). MC-ICP-MS was used to determine the <sup>230</sup>Th age of the eight samples. The details of the instrumental parameters were described by Wang et al. (2016).

## 5 Results

Petrographic investigations of two breccia hand specimens facilitated the discrimination of textures and fabrics in each sample (Fig. 3). All thin sections of breccia samples showed no traces of dissolution or redeposition and were thus considered suitable materials for U–Th dating.

The results of <sup>230</sup>Th/U dating are presented in Table 1. In general, the secondary calcium carbonate ages produced realistic radiometric ages, with samples possessing high <sup>238</sup>U contents and mostly high <sup>230</sup>Th/<sup>232</sup>Th activity ratios. Although the <sup>232</sup>Th content in BHJT4 was high, which may have been caused by detrital contamination, the <sup>230</sup>Th/<sup>232</sup>Th ratio was still greater than 20. Accordingly, the obtained ages have moderate to low uncertainties. For the breccia samples, the BHJT2-1 age was 200,677 ± 1377 a, the BHJT2-2 age was 19,577 ± 2580 a, and the BHJT4 age was 205,486 ± 14,259 a (Fig. 3e–h). The age of the bottom of the BHJT3BS stalagmite was 238,144 ± 3715 a, while the ages at the top were 221,253 ± 5595 a (BHJT3BS2) and 212,622 ± 5625 a (BHJT3BS3) (Fig. 3l). The ages of stalagmite BHJT3CS ranged from 212,255 ± 3425 a (BHJT3CS1) to 203,253 ± 3471 a (BHJT3CS2) (Fig. 3k).

## 6 Discussion

### 6.1 Age of the colluvium

When the underground river was at the elevation of the platform of Huajiang village, the river eroded the tunnel laterally, continuously expanding the underground cave chamber, which provided storage space for large-scale and possibly multiple collapses. Eventually, a large number of colluvial deposits accumulated at the bottom of the original

underground river channel. Due to the loose structure of breccia, cementation can occur if infiltrating water is supersaturated concerning carbonate (Piccini et al. 2003). Thick secondary calcium carbonate deposits were formed in some fractures, and these deposits have laminae similar to cave flowstones (Fig. 3d–h). According to the dates provided, cementation was probably completed within a very short time after the collapse (approximately 200 ka). Because of case hardening, the interblock porosity of the breccia was reduced, significantly lowering the possibility of later dissolution (Ford and Williams 2007). Therefore, the secondary calcium carbonate deposits in the breccia fractures were probably not redeposited. The lack of redissolution/redeposition effects promoted a closed system for uranium, facilitating reliable U-series dating. The cementation time of the breccia represents the time of the collapse event. Stalagmites are products of caves; therefore, the ages of the stalagmites indicate when Huajiang Canyon was still in a cave environment. Karst areas in Southwest China generally lack sufficient surface sediments (Liu et al. 2013). Consequently, the evolutionary history of the Guizhou Plateau is not clear, which greatly restricts our understanding of the formation and evolutionary processes of the Guizhou karst landforms. This study attempted to overcome this limitation by determining the cementation age of karst breccia cement.

### 6.2 Causes of cave collapse in the Huajiang Grand Canyon

Geomorphological observations and the presence of extensive breccia deposits suggest the occurrence of a large-scale collapse in Huajiang Canyon related to previous subterranean karst drainage. The stability of caves is limited (Ford and Williams 2007), especially in areas characterized by rapid tectonic uplift. When the cavern in the study location was enlarged to a certain volume, it began to gradually collapse, exposing the underground features at the surface. Stalagmite BHJT3BS, which is currently at the surface, clearly supports this scenario. When the tiankeng first formed, it was likely ring-shaped. Its original morphology was eventually obliterated by additional collapses. At present, a residual vertical cliff remains on the western side of Huajiang gorge (Fig. 2).

Cave collapse in the Huajiang Grand Canyon was possibly triggered by a combination of the following tectonic and geological characteristics of the area:

- Rapid uplift of the Yunnan–Guizhou Plateau since the Cenozoic is related to the tectonics of the Qinghai–Tibetan Plateau, which has been in an overall uplift tectonic environment. This has caused ongoing base level deepening, which promotes the formation of

**Table 1** Radiometric (U–Th) ages of karst breccia samples from Huajiang Canyon

Sample	$^{238}\text{U}$ (ppb)	$^{232}\text{Th}$ (ppt)	$^{230}\text{Th}/^{232}\text{Th}$ (atomic $\times 10^{-6}$ )	$\delta^{234}\text{U}^*$ (measured)	$^{230}\text{Th}/^{238}\text{U}$ (activity)	$^{230}\text{Th}$ age (yr) (uncorrected)	$^{230}\text{Th}$ age (yr) (corrected)	$\delta^{234}\text{U}_{\text{initial}}^{**}$ (corrected)	$^{230}\text{Th}$ age (yr) BP*** (corrected)
BHJT2-1	$565.7 \pm 0.50$	$5154 \pm 103$	$1540.3 \pm 30.9$	$7.5 \pm 1.5$	$0.8512 \pm 0.0012$	$201,006 \pm 1368$	$200,744 \pm 1377$	$13 \pm 3$	$200,677 \pm 1377$
BHJ T2-2	$460.7 \pm 0.40$	$51,026 \pm 1022$	$128.2 \pm 2.6$	$21.4 \pm 1.5$	$0.8609 \pm 0.0013$	$198,997 \pm 1340$	$195,844 \pm 2580$	$37 \pm 3$	$195,777 \pm 2580$
BHJT4	$80.7 \pm 0.10$	$52,849 \pm 1059$	$22.9 \pm 0.5$	$34.2 \pm 2.3$	$0.9108 \pm 0.0024$	$225,156 \pm 2786$	$205,554 \pm 14,259$	$61 \pm 5$	$205,486 \pm 14,259$
BHJT3BS1	$347 \pm 0.46$	$44,287 \pm 888$	$118.9 \pm 2.4$	$25.5 \pm 1.8$	$0.9200 \pm 0.0021$	$241,809 \pm 2806$	$238,214 \pm 3715$	$50 \pm 4$	$238,144 \pm 3715$
BHJT3BS2	$605 \pm 1.00$	$147,354 \pm 2954$	$61.0 \pm 1.2$	$22.1 \pm 2.1$	$0.9012 \pm 0.0022$	$228,346 \pm 2746$	$221,324 \pm 5595$	$41 \pm 4$	$221,253 \pm 5595$
BHJT3BS3	$482 \pm 1.00$	$117,894 \pm 2362$	$60.0 \pm 1.2$	$21.8 \pm 1.8$	$0.8904 \pm 0.0029$	$219,759 \pm 2745$	$212,693 \pm 5625$	$40 \pm 3$	$212,622 \pm 5625$
BHJT3CS1	$815 \pm 1.00$	$115,960 \pm 2324$	$102.5 \pm 2.1$	$20.8 \pm 1.5$	$0.8850 \pm 0.0019$	$216,390 \pm 1938$	$212,326 \pm 3425$	$38 \pm 3$	$212,255 \pm 3425$
BHJT3CS2	$570 \pm 1.00$	$83,500 \pm 1674$	$97.9 \pm 2.0$	$17.7 \pm 1.7$	$0.8696 \pm 0.0019$	$207,537 \pm 1855$	$203,324 \pm 3471$	$31 \pm 3$	$203,253 \pm 3471$

\*  $\delta^{234}\text{U} = ([^{234}\text{U}/^{238}\text{U}]_{\text{activity}} - 1) \times 1000$ . \*\*  $\delta^{234}\text{U}_{\text{initial}}$  was calculated based on the  $^{230}\text{Th}$  age (T), i.e.,  $\delta^{234}\text{U}_{\text{initial}} = \delta^{234}\text{U}_{\text{measured}} \times e^{234 \times T}$ . Corrected  $^{230}\text{Th}$  ages assume an initial  $^{230}\text{Th}/^{232}\text{Th}$  atomic ratio of  $(4.4 \pm 2.2) \times 10^{-6}$ . This value is for material at secular equilibrium, with a bulk earth  $^{232}\text{Th}/^{238}\text{U}$  value of 3.8. The errors are arbitrarily assumed to be 50%. \*\*\*B.P. denotes “before present”, where “present” is defined as the year 1950 A.D.

underground rivers (Sweeting 1995). The Huajiang Grand Canyon is located west of the Zhenfeng thrust fault. The western side is the hanging wall of the thrust fault, and its tectonic uplift significantly increases the river drop on both sides of the fault, resulting in accelerated river downcutting.

- From a geological perspective, the Huajiang Grand Canyon is carved into dolomite. In the past, the dissolution rate of dolomite was believed to be lower than that of limestone. However, a recent study on the chemical denudation rate of dolomite in the Shibing area of Guizhou Province showed that the dolomite chemical denudation rate is similar to or even higher than that of limestone under a similar climate (He et al. 2018). Importantly, dolomite is prone to collapse if a static equilibrium is compromised (Luo et al. 2019). Therefore, physical collapse is particularly important for the formation of dolomite caves. The platform around Huajiang village is characterized by abundant collapse breccia deposits, which suggest the occurrence of a large-scale collapse event. U-series dating analysis of breccia cement samples from different parts and altitudes in the tiankeng showed that the samples experienced approximately synchronous cementation. This implies that the collapse leading to the formation of the tiankeng was completed in one main event or at least within a short period. There are no younger large-scale colluvial deposits above the breccia, except for recent small-scale colluvial deposits found under the cliff at the Huajiang Tiankeng. Minor collapse processes may continue, but the collapse event that played a decisive role in the landscape of Huajiang gorge occurred  $\sim 200$  ka. In addition, many ancient stalagmites were observed on the Huajiang platform (Fig. 3). As stalagmites do not occur at the surface, the development of the gorge can certainly be attributed to cave collapse.

### 6.3 Evolutionary processes of Huajiang Canyon

According to field observations during the geomorphological survey and based on chronological data, the development and evolutionary process of Huajiang Canyon can be divided into four stages as follows:

- During the Early Pleistocene, surface rivers flowed through wide valleys in the Huajiang gorge (Stage 1 in Fig. 4), and the karst system had not yet formed. Previous studies have also indicated the formation of wide valleys in the upper reaches during the early Pleistocene (Li 2001).
- Subsequently, due to the tectonic uplift of the western side of the Zhenfeng Fault, the Beipan River base level

dropped, promoting underground excavation. The underground river channel likely continued to erode laterally, continuously expanding the tunnel and forming large caverns, which favoured the occurrence of collapse and provided storage space for the accumulation of colluvium (Stage 2 in Fig. 4). At this stage, stalagmites formed at the bottom of the newly formed caves (Fig. 4). These stalagmites stopped growing approximately 203 ka.

- The space in the underground cave continuously expanded, leading to one or more collapse events. According to the U-series dating of the cement, some collapses occurred  $\sim 200$  ka BP. Subsequently, the underground rivers were exposed as surface rivers, and colluvium accumulated at the bottom of the tiankeng (Stage 3 in Fig. 4).
- After colluvial deposition, with continuous tectonic uplift, the river underwent rapid incision. From the bottom of the colluvium, at altitudes of 685 to 500 m (current height of the river), the incision depth reached 185 m, forming a deep canyon (Stage 4 in Fig. 4). Since 200 ka, the river incision rate has reached 0.92 m/ka. This result is close to the research result of the incision rate of the Nizhu River canyon in the upper reaches of the Beipan River (Fan et al. 2021). Crustal uplift is a necessary condition for the formation of deep canyons (Hu et al. 2016). Rapid downcutting of the Huajiang gorge by the Beipan River was mainly controlled by the activity of the Zhenfeng Fault, which was attributable to the acceleration of tectonic uplift on the western side of the Zhenfeng Fault.

## 7 Conclusion

In this study, the formation and evolutionary processes of Huajiang Grand Canyon were explored. Field surveys were conducted, and analyses of samples collected from Huajiang Canyon in the middle reaches of the Beipan River were performed. The main findings can be summarized as follows:

- A large number of collapsed breccias were preserved on the platform in the residual tiankeng of the Huajiang Grand Canyon on the Beipan River. U-series dating of two stalagmites found at the surface attested to the presence of an underground environment between 238 and 203 ka. In contrast, the ages of breccia cements revealed that a large-scale collapse event occurred in Huajiang Grand Canyon at least  $\sim 200$  ka.
- Collapse is a very common geomorphic process in karst areas, especially under a tectonic background of integral uplift, such as that of the Yunnan–Guizhou



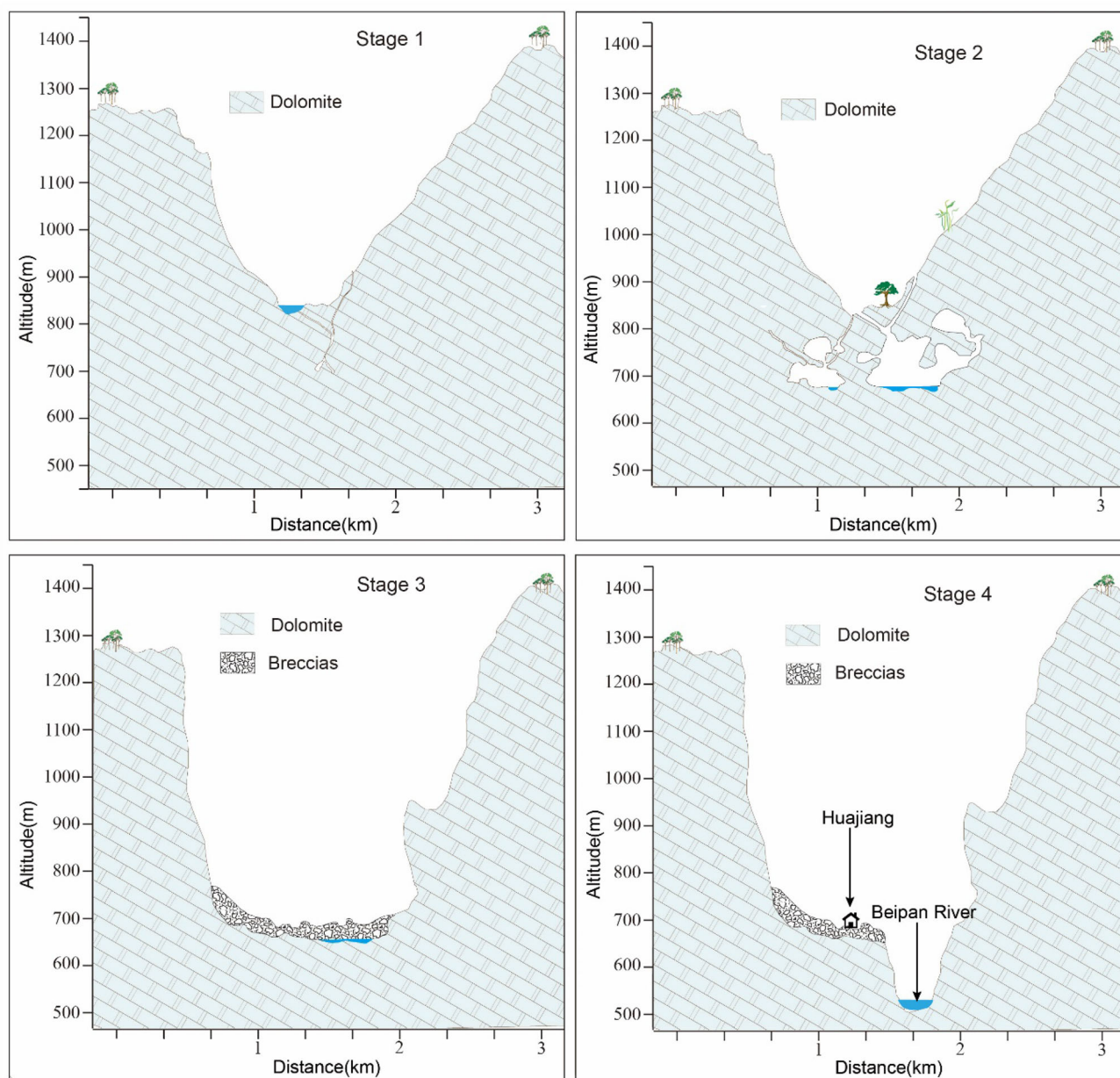


**Fig. 4** Evolutionary model of Huajiang Canyon and the Beipan River

Plateau. Collapses frequently occur in karst underground caves and canyons. Many cave collapses lead to the formation of skylights and tiankengs, and continuous collapse leads to the formation of canyons. Therefore, the collapse process is a common and very important formation mechanism in the evolution of karst gorges.

- Collapse phenomena and associated colluvium are very common in karst areas, but their ages of occurrence are difficult to determine. By U-series chronology testing of collapse breccia cement, the time of collapse can be accurately determined. This approach, combined with

analyses of cave-specific deposits such as stalagmites, may provide an effective means for studying canyon development and determining the ages of tiankeng formations in karst areas.

**Acknowledgements** We thank Ming Tan, Paul W. Williams, Yu Liu, Changshun Song, Wenlong Zhou, Taiping Ye and Zongmeng Li for helpful discussions on various aspects of this work. This research was funded by the National Natural Science Foundation of China (Grant:42061001, 41501006); The Science and Technology Foundation of Guizhou Province (Grant: Qianke Jichu-ZK[2021]190); Natural science research funding project of Guizhou Provincial Department of Education (Grant: Qian Jiao KY[2021]036).

## 468 Declaration

469 **Conflict of interest** On behalf of all authors, the corresponding  
470 author states that there is no conflict of interest.

## 471 References

- 472 Abbott L, Lundstrom C, Traub C (2015) Rates of river incision and  
473 scarp retreat in eastern and central grand canyon over the past  
474 half million years: evidence for passage of a transient knickzone.  
475 *Geosphere* 11(3):638–659
- 476 Alexander K (2005) Cave un-roofing as a large-scale geomorphic  
477 process. *Cave Karst Sci* 32(2–3):93–98
- 478 Ambert P, Nicod J (1981) Sur quelques karsts de Serbie, au voisinage  
479 du Danube. Leurs rapports avec l'évolution du bassin pannonien.  
480 *Revue Géographique De L'est* 21(4):235–249
- 481 An D, Zhou Z, Xue BQ, Yang E, Fan B, Zhu C et al (2019) Spatial  
482 distribution characteristics and the geomorphological evolution  
483 process of the Jiudongtian cave system in Guizhou Province.  
484 *Carsologica Sinica* 6:967–976
- 485 Anthony D (2012) Multilevel caves and landscape evolution. In:  
486 *Encyclopedia of Caves (Second Edition)* pp 528–531
- 487 Chen J, Edwards R, Wasserburg G (1986)  $^{238}\text{U}$ ,  $^{234}\text{U}$  and  $^{232}\text{Th}$  in  
488 seawater. *Earth Planet Sci Lett* 80(3–4):241–251
- 489 Cheng H, Edwards R, Sinha A, Christoph S, Liang Y, Shitao C,  
490 Hellstrom J, Wang Y, Kong X, Spötl C, Wang X, Alexander J  
491 et al (2013) Improvements in  $^{230}\text{Th}$  dating,  $^{230}\text{Th}$  and  $^{234}\text{U}$  half-  
492 life values, and U-Th isotopic measurements by multi-collector  
493 inductively coupled plasma mass spectrometry. *Earth Planet Sci*  
494 *Lett* 371–372:82–91
- 495 Cheng H, Edwards R, Sinha A, Christoph S, Liang Y, Shitao C,  
496 Megan K, Gayatri K, WX, Li X, Kong X, Wang Y, Ning Y,  
497 Zhang H et al (2016) The Asian monsoon over the past 640,000  
498 years and ice age terminations. *Nature* 534(7609):640–646
- 499 Clark M, Royden L, Whipple K, Burchfiel B, Zhang X, Tang W et al  
500 (2006) Use of a regional, relict landscape to measure vertical  
501 deformation of the eastern tibetan plateau. *J Geophys Res Earth*  
502 *Surf* 111:F03002. <https://doi.org/10.1029/2005JF000294>
- 503 Columbu A, Waele J, Forti P, Montagna P, Drysdale R et al (2015)  
504 Gypsum caves as indicators of climate-driven river incision and  
505 aggradation in a rapidly uplifting region. *Geology*  
506 43(6):539–542
- 507 Columbu A, Audra P, Gázquez F, D'Angeli IM, Bigot JY, Koltai G,  
508 Chiesa R, Yu TL, Hu HM, Shen CC et al (2021) Hypogenic  
509 speleogenesis, late stage epigenic overprinting and condensa-  
510 tion-corrosion in a complex cave system in relation to landscape  
511 evolution (Toirano, Liguria, Italy). *Geomorphology* 376:107561
- 512 Columbu A, Chiarini V, De Waele J, Drysdale R, Woodhead J,  
513 Hellstrom J, Forti P et al (2017) Late quaternary speleogenesis  
514 and landscape evolution in the northern Apennine evaporite  
515 areas. *Earth Surf Proc Land* 42(10):1447–1459
- 516 De Waele J, D'Angeli IM, Bontognali T, Tuccimei P, Scholz D,  
517 Jochum KP, Columbu A, Bernasconi SM, Fornós JJ, González  
518 ERG, Tisato N (2018) Speleothems in a north Cuban cave  
519 register sea level changes and Pleistocene uplift rates. *Earth Surf*  
520 *Proc Land* 43:2313–2326
- 521 Edwards L, Chen J, Wasserburg G (1987)  $^{238}\text{U}$ – $^{234}\text{U}$ – $^{230}\text{Th}$ – $^{232}\text{Th}$   
522 systematics and the precise measurement of time over the past  
523 500,000 years. *Earth Planet Sci Lett* 81(2–3):175–192
- 524 Fabre G, Nicod J (1978) Niveaux de base actuels dans les principaux  
525 canyons du Languedoc oriental et des Plans de provence. *IJS*  
526 10(3):279–291
- Fan YL, Liu JJ, Zhu KW, Li HB, Zou XX (2021) Study on river  
527 downcutting rate in Karst Canyon—a case study of Nizhu River  
528 Grand Canyon in Beipan River. *Q Sci* 41(6):1558–1564
- Fan YL, Pan BT, Hu ZB, Ren DY, Chen QW, Liu FL, Li ZM (2018)  
529 An analysis of tectonic geomorphologic characteristics of the  
530 Beipanjiang basin in the Yunnan-Guizhou plateau. *Adv Earth*  
531 *Sci* 33(7):751–761
- Ford D (1973) Development of the canyons of the South Nahanni  
532 river NWT. *Canad J Earth Sci* 10(3):366–378
- Ford D, Williams P (2007) Karst hydrogeology and geomorphology.  
533 Wiley, Chichester, pp 99–134, 265–270
- Germanoski D, Ritter D (1988) Tributary response to local base level  
534 lowering below a dam. *Regul Rivers Res Manage* 2(1):11–24
- Granger D, Fabel D, (2012) Cosmogenic isotope dating of cave sediments.  
535 In: *Encyclopedia of Caves (Second Edition)*, pp 172–177
- He J, Xia S, Zeng C, Di Y, Liu M, Lan J, Xiao H, Zhu H, Zeng Q  
536 et al (2018) Chemical denudation rate in typical humid  
537 subtropical dolomite catchments: a case study in the Huangzhou  
538 River basin, Shibing. *Guizhou Earth Environ* 46(3):274–281
- Hill C, Eberz N, Buecher R (2008) A karst connection model for  
539 Grand Canyon, Arizona, USA. *Geomorphology* 95:316–334
- Hu Z, Pan B, Guo L, Vandenberghe J, Hu X et al (2016) Rapid fluvial  
540 incision and headward erosion by the yellow river along the  
541 jinshaan gorge during the past 1.2 ma as a result of tectonic  
542 extension. *Quatern Sci Rev* 133:1–14
- Karlstrom K, Lee J, Kelley S, Crow R, Crosse L, Young R, Lazear  
543 G, Beard L, Ricketts J, Fox M et al (2014) Formation of the  
544 grand canyon 5 to 6 million years ago through integration of  
545 older palaeocanyons. *Nat Geosci* 7(3):239–244
- Li X (2001) An analysis of physiographic stage in the karst region of  
546 Guizhou Plateau. *Guizhou Geol* 3:182–186
- Liu Y, Wang S, Xu S, Liu X, Fabel D, Zhang X, Luo W, Cheng A  
547 et al (2013) New evidence for the incision history of the  
548 Liuchong River, Southwest China, from cosmogenic  $^{26}\text{Al}/^{10}\text{Be}$   
549 burial ages in cave sediments. *J Asian Earth Sci* 73:274–283
- Luo S, Li P, Chen W, WY, Ouyang Z, Qin X et al (2019) Study on  
550 development mechanism and evolution of Shuanghe Cave  
551 system in Suiyang, Guizhou. *J Chongqing Normal Univ Nat*  
552 *Sci Edition* 36(1):111–118
- Meng Q, Shen H, Mao L, Liang W, Zhao Z, Liang Z, Lai M, Huang  
553 B, Li S, He M, Shan J et al (2017) Determination of exposure  
554 age of Tiankeng, Leye county of Guangxi by accelerator mass  
555 spectrometry. *J Guangxi Normal Univ Nat Sci Edition*  
556 35(1):16–20
- Michelena M, Kilian R, Baeza O, Rios F, Rivero M, Mesa J,  
557 González V, Ordoñez A, Langlais B, Rocca M, Acevedo R et al  
558 (2020) The formation of a giant collapse caprock sinkhole on the  
559 Barda Negra plateau basalts (Argentina) Magnetic, mineralogical  
560 and morphostructural evidences. *Geomorphology* 367:107297
- Nicod J (1997) The karstic canyons, geomorphological problems and  
561 new directions (particularly in mediterranean and tropical lands).  
562 *Quaternaire* 8(2):71–89
- Piccini L, Drysdale R, Heijnis H (2003) Karst morphology and cave  
563 sediments as indicators of the uplift history in the Alpi Apuane  
564 (Tuscany, Italy). *Quatern Int* 101–102:219–227
- Polyak V, Hill C, Asmerom Y (2008) Age and evolution of the Grand  
565 Canyon revealed by U-Pb dating of water table-type speleothems.  
566 *Science* 319:1377–1380
- Sasowsky ID (1998) Determining the age of what is not there. *Science*  
567 279(5358):1874
- Shen C, Edwards R, Cheng H, Dorale J, Thomas R, Moran S,  
568 Weinstein S, Edmonds H et al (2002) Uranium and thorium  
569 isotopic and concentration measurements by magnetic sector  
570 inductively coupled plasma mass spectrometry. *Chem Geol*  
571 185(3–4):165–178

- Shui W, Chen Y, Wang Y, Su Z, Zhang S et al (2015) Origination, study progress and prospect of Karst Tiankeng research in China. *Acta Geogr Sin* 70(3):431–446
- Sweeting M (1995) Karst in China. Its Geomorphology and Environment/Springer V. pp: 265
- Szczygiel J, Golicz M, Hercman H, Lynch E et al (2018) Geological constraints on cave development in the plateau- gorge karst of south china (wulong, chongqing). *Geomorphology* 304:50–63
- Tapponnier P (2001) Oblique stepwise rise and growth of the tibet plateau. *Science* 294(5547):1671–1677
- Telbisz T, Stergiou C, Mindszenty A (2019) Karst features and related social processes in the region of the Vikos gorge and Tymphi mountain (Northern Pindos National Park, Greece). *Acta Carsologica* 48(1):29–42
- Waltham T (2005) Collapse processes at the Tiankengs of Xingwen. *Cave and Karst Science* 32(2–3):107–110
- Waltham T (2015) Large collapse sinkholes, old and new, in the Obruk Plateau, Turkey. *Cave Karst Sci* 42:125–130
- Wang F, Li H, Zhu R, Qin F et al (2004) Late quaternary downcutting rates of the Qianyou River from U/Th speleothem dates, Qinling mountains China. *Q Res* 62(2):194–200
- Wang L, Ma Z, Cheng H, Duan W, Xiao J et al (2016) Determination of  $^{230}\text{Th}$  dating age of uranium-series standard sample by multiple collector inductively coupled plasma mass spectrometry. *J Chin Mass Spectrometry Soc* 37(3):262–272
- Wang L, Ma Z, Sun Z, Wang Y, Wang X, Cheng H, Xiao J et al (2017) U concentration and  $^{234}\text{U} / ^{238}\text{U}$  of seawater from the Okinawa Trough and Indian Ocean using MC-ICPMS with SEM protocols. *Mar Chem* 196:71–80
- Wang P, Scherler D, Liu Z, Mey J, Avouac J, Zhang Y, Shi D et al (2014) Tectonic control of Yarlung Tsangpo gorge revealed by a buried canyon in southern tibet. *Science* 346(6212):978–981
- Wei Y, Li C, Chen W, Wu Z, Luo Q, Zhai X, Bai B et al (2019) Characteristics and formation and evolution analysis of the karst landscape of Fengjie Tiankeng Difeng Scenic Area. *Chongqing Acta Geoscientica Sinica* 40(5):747–766
- Zhang Y, Mo Z (1982) The origin and evolution of Orange fall. *Acta Geogr Sin* 49(3):303–316
- Zhu X, Chen W (2005) Tiankengs in the karst of China. *Cave Karst Sci* 32(2–3):55–66
- Zhu X, Waltham T (2005) Tiankeng definition and description. *Cave Karst Sci* 32(2–3):75–79

Journal : **11631**

Article : **510**

## Author Query Form

**Please ensure you fill out your response to the queries raised below and return this form along with your corrections**

Dear Author

During the process of typesetting your article, the following queries have arisen. Please check your typeset proof carefully against the queries listed below and mark the necessary changes either directly on the proof/online grid or in the 'Author's response' area provided below

Query	Details Required	Author's Response
<a href="#">AQ1</a>	As keywords are mandatory for this journal, please provide 3–6 keywords.	